Molecular Therapy
Nucleic Acids
Original Article

Gain of Metabolic Benefit with Ablation of miR-149-3p from Subcutaneous Adipose Tissue in Diet-Induced Obese Mice

Shasha Zheng,[1,4] Shanjun Guo,[1,4] Gongrui Sun,[1,4] Yanteng Shi,[1] Zhe Wei,[1] Yuhang Tang,[1] Fangfang He,[1] Chenke Shi,[1] Peng Dai,[1] Hoshun Chong,[2] Isabella Samuelson,[3] Ke Zen,[1] Chen-Yu Zhang,[1] Yujing Zhang,[1] Jing Li,[1] and Xiaohong Jiang[1]

[1]State Key Laboratory of Pharmaceutical Biotechnology, NJU Advanced Institute for Life Sciences (NAILS), School of Life Sciences, Nanjing University, Nanjing, Jiangsu 210093, China; [2]Department of Thoracic and Cardiovascular Surgery, Nanjing Drum Tower Hospital, The Affiliated Hospital of Nanjing University Medical School, Nanjing, China; [3]University of Cambridge Metabolic Research Laboratories, Wellcome Trust-MRC Institute of Metabolic Science, Addenbrooke's Hospital, Cambridge CB2 0QQ, UK

The global rise in obesity has become a public health crisis. During the onset of obesity, disrupted catecholamine signals have been described to contribute to excess fat accumulation, however, the molecular and metabolic change of subcutaneous adipose tissue (SAT) upon chronic high-fat feeding has rarely been investigated. Here, we show that chronic high-fat feeding caused a significant decrease in the expression of thermogenic genes and acquisition of partial deleterious features of visceral fat in SAT. Upregulated miR-149-3p was involved in this obesity-induced "visceralization" of SAT via inhibiting PRDM16, a master regulator that promoted SAT thermogenesis. Reduction of miR-149-3p significantly increased PRDM16 expression in SAT, with improved whole-body insulin sensitivity, decreased SAT inflammation, and liver steatosis in high-fat fed mice. These findings provided direct evidence of the anti-obese and anti-diabetic effect of PRDM16 in the obese background for the first time and identified that miR-149-3p could serve as a therapeutic target to protect against diet-induced obesity and metabolic dysfunctions.

INTRODUCTION

The global rise in obesity has become a public health crisis.[1] Excess body fat can increase the risk for many chronic diseases, like type 2 diabetes, cardiovascular disease, liver disease, and other metabolic syndromes.[2–4] Recent studies revealed that approximately 20% of many common cancers are also caused by excess body fat accumulation.[5] Thus, feasible strategies to reduce adiposity are urgently needed. Because a western diet and sedentary lifestyle result in an imbalance between energy intake and expenditure,[6] nonsurgical therapy to increase energy expenditure could be an efficient approach to overcome obesity.

The main function of white adipocytes is to store excess energy as triglycerides, whereas brown and beige adipocytes are specialized to oxidize chemical energy to produce heat, which constitutes a natural defense against hypothermia and obesity.[7] Due to the relatively small amount of classic brown adipocytes in adult human beings, the induction of subcutaneous white adipocytes into the intermediate category of beige adipocytes, also known as "browning" of white adipocytes, has become a research focus.[8] It has been reported that activation of the multilocular smaller beige adipocytes in subcutaneous adipose tissue (SAT) protected mice and humans from diet-induced obesity and related metabolic complications, such as insulin resistance.[9,10] On the other hand, previous studies found that the percentage of large white adipocytes (>5,000 μm^2) was significantly higher in the subcutaneous depot of obesity-prone mice,[11] indicating the loss of the metabolic benefit of SAT. Therefore, activating the beige adipocytes in SAT may pave the way for improved therapeutic strategies to help combat metabolic disorders.

Although β-adrenergic agonists and other hormone-like stimuli were shown to be able to induce SAT "browning,"[12,13] physiological cold stress is still the most prominent way to activate the multilocular beige adipocytes.[14] Thus, developing therapies aimed at increasing beige adipocyte number requires detailed mechanistic understanding. PR-domain-containing 16 (*Prdm16*) is a critical transcriptional factor that powerfully regulates beige adipocyte differentiation and thermogenic gene expression in SAT.[15] Interestingly, depot-dependent effects were observed in mice that overexpress *Prdm16*, probably due to the

Received 16 March 2019; accepted 24 July 2019;
https://doi.org/10.1016/j.omtn.2019.07.024.

[4]These authors contributed equally to this work.

Correspondence: Xiaohong Jiang, PhD, State Key Laboratory of Pharmaceutical Biotechnology, NJU Advanced Institute for Life Sciences (NAILS), School of Life Sciences, Nanjing University, 163 Xianlin Road, Nanjing, Jiangsu 210093, China.
E-mail: xiaohongjiang@nju.edu.cn
Correspondence: Jing Li, PhD, State Key Laboratory of Pharmaceutical Biotechnology, NJU Advanced Institute for Life Sciences (NAILS), School of Life Sciences, Nanjing University, 163 Xianlin Road, Nanjing, Jiangsu 210093, China.
E-mail: jingli220@nju.edu.cn
Correspondence: Yujing Zhang, PhD, State Key Laboratory of Pharmaceutical Biotechnology, NJU Advanced Institute for Life Sciences (NAILS), School of Life Sciences, Nanjing University, 163 Xianlin Road, Nanjing, Jiangsu 210093, China.
E-mail: yjzhang@nju.edu.cn

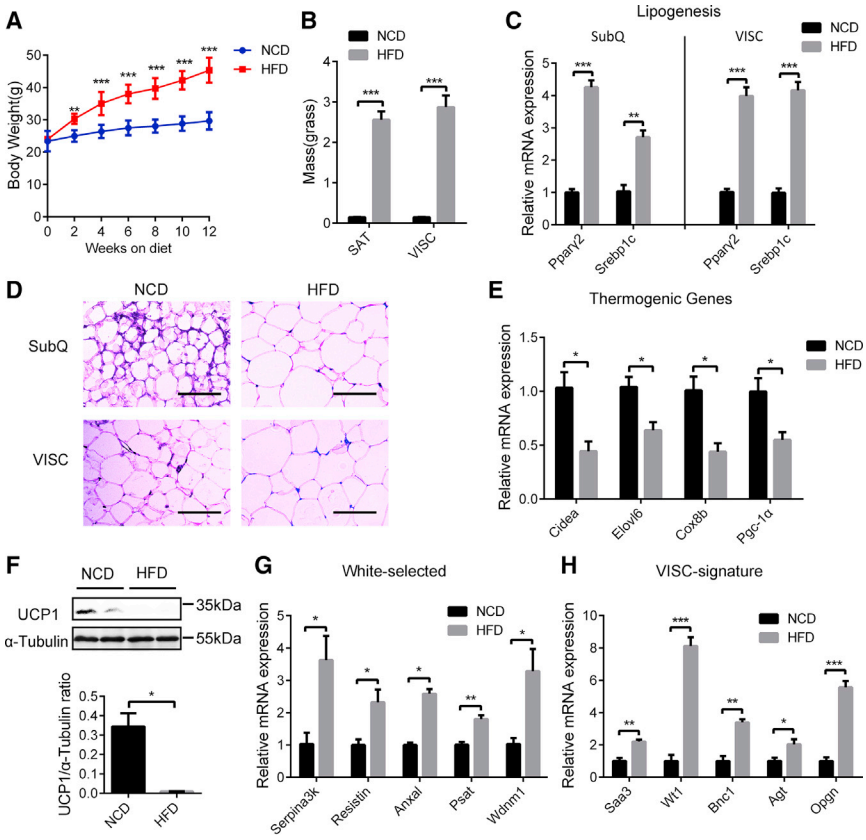

Figure 1. High-Fat Diet Induces the Partial Visceral-like Switches of SAT

(A–H) Mice were fed on HFD or NCD for 12 weeks. (A) Body weights of mice on NCD or HFD. (B) Weights of fat pads from mice (n = 8). (C) Normalized expression of lipogenesis genes in subcutaneous and visceral adipose tissue from mice fed on NCD or HFD (n = 8). (D) H&E staining of SAT and visceral (VISC) adipose tissue. Scale bars: 100 μm. (E) Normalized expression of thermogenic genes in SAT (n = 8). (F) Western blot analysis of UCP1 protein level in SAT. (G and H) Normalized expression of white adipose tissue-selective genes (G) and visceral white adipose tissue-selective genes (H) in SAT from mice fed on NCD or HFD. *p < 0.05, **p < 0.01, ***p < 0.001.

differential stability of the protein in subcutaneous and visceral fat.[16] Of note, increased expression of *Prdm16* markedly promoted beige development in SAT, which protected mice against diet-induced metabolic diseases.[15] By contrast, ablation of *Prdm16* caused a profound loss of beige cell function in SAT, leading to aggravated obesity and hepatic steatosis.[17] Thus, identifying signaling molecules that transcriptionally or post-transcriptionally regulate *Prdm16* may offer new targets for clinical applications. Mechanistic studies revealed that the anti-diabetic drug Rosiglitazone can convert white to beige adipocytes through stabilizing PRDM16 expression.[18] However, owing to its apparent association with increased risks of heart attack and other severe side effects, Rosiglitazone is not ideal for targeting PRDM16 *in vivo*.

MicroRNAs (miRNAs) are small non-coding RNA molecules that negatively regulate gene expression through targeting the 3′ UTR of mature mRNA.[19] Recently, the role of miRNAs in adipocyte function has received significant attention.[8,20] By generating mice with an adipose tissue-specific knockout of Dicer, a major endoribonuclease for miRNA maturation, Mori et al.[21] observed significant "whitening" of interscapular brown adipose tissue (BAT), suggesting the necessity of normal miRNA processing for maintaining adipose function. Notably, several miRNAs have been found to play essential roles in classic brown and beige cell adipogenesis.[22–24] For example, miR-193b/365 cluster, which is co-localized on chromosome 16, regulated brown fat differentiation by targeting Runx1t1.[25] In addition, miR-196a mediated SAT browning via inhibition of Hoxc8, which could repress the expression of the brown adipogenic marker C/EBPβ.[26] Moreover, the muscle-enriched miR-133 was shown to impair both brown and beige cell development by targeting *Prdm16*. Collectively, these studies indicate that miRNAs are important signaling molecules to promote beige cell function.

Here, we reported that the expression of miR-149-3p was elevated in SAT of high-fat fed mice. The deregulated expression of miR-149-3p caused an acquisition of partial visceral like features of SAT, along with reduced thermogenic capability through targeting *Prdm16* in obese mice. Reduction of miR-149-3p expression in SAT significantly improved diet-induced glucose intolerance and hepatic steatosis via increasing energy expenditure.

RESULTS

High-Fat Diet Induces the Acquisition of Partial Visceral-like Features of SAT

Although it is well known that visceral fat deposition leads to a series of metabolic abnormalities, whether a high-fat diet (HFD) also influences the molecular and functional characteristics of SAT is still debated.[27–29] To investigate the effect of HFD on SAT metabolism, we placed mice on HFD for 12 weeks. As shown in Figures 1A and 1B, compared with mice fed on normal chow diet (NCD), HFD feeding not only caused increased body weight but also significantly elevated the weight of visceral epididymal white adipose tissue (WAT), as well as the subcutaneous inguinal fat depot. Consistently, the mRNA levels of two main lipogenic transcription factors, *Pparγ2* and *Srebp1c*, were markedly upregulated in both epiWAT and ingWAT, indicating increased lipogenesis in both visceral and subcutaneous fat (Figure 1C). Interestingly, histological analysis showed that the average cell volume was much larger in SAT of HFD-fed mice, which resembles the epiWAT (Figure 1D). A defining feature of SAT is its higher capacity for thermogenesis compared with visceral WAT. Hence, the mRNA levels of thermogenic-associated genes were accessed in SAT. As shown in Figure 1E,

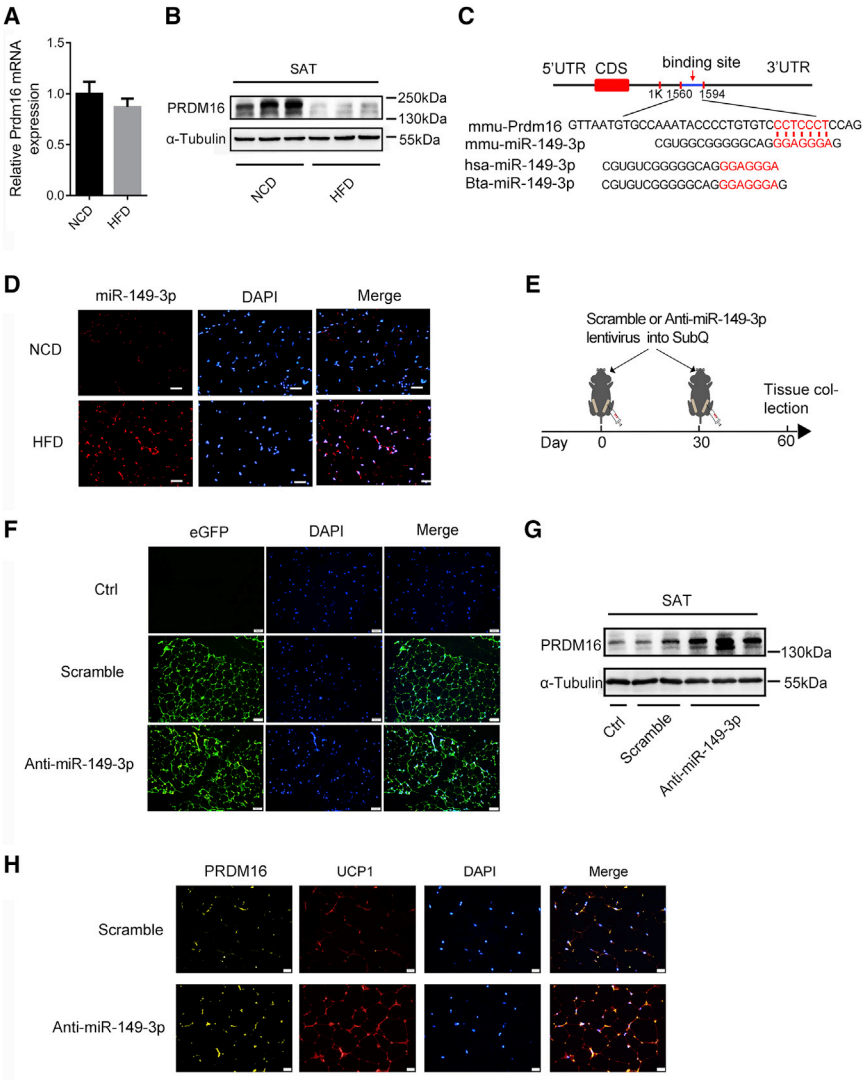

Figure 2. miR-149-3p Decreases PRDM16 Expression in SAT upon High-Fat Feeding

(A and B) Analysis of PRDM16 mRNA (A) and protein levels (B) in the SAT adipose tissue from mice fed on NCD or HFD. (C) Schematic descriptions of the putative duplexes formed by miR-149-3p with the 3′ UTR of PRDM16. (D) FISH for miR-149-3p in the SAT from mice fed on NCD or HFD. Scale bars: 50 μm. (E–H) Lentiviral vector (LV) containing scrambled control (scramble) or antisense-miR-149-3p (anti-miR-149-3p) or PBS (ctrl) were used for SAT adipose tissue infection in male mice (n = 8). (E) Schematic of the experimental protocol. (F) Appearance of GFP in SAT adipose tissue of mice infected with LV-scramble or LV-anti-miR-149-3p or PBS. Nuclei were stained with DAPI (blue). Scale bars: 100 μm. (G) Western blot analysis of PRDM16 protein level in the three groups of SAT. (H) Immunofluorescence analysis of UCP1 and PRDM16 expression in SAT adipose tissue of mice infected with LV-scramble or LV-miR-149-3p. Scale bars: 20 μm. *$p < 0.05$, **$p < 0.01$, ***$p < 0.001$.

Cidea, *Elovl6*, *Cox8b*, and *Pgc-1α* were markedly decreased in the inguinal SAT of HFD-fed mice. Immunoblotting analysis also revealed that a certain amount of UCP1 was readily observed in the ingWAT of mice fed NCD, whereas the UCP1 was almost undetectable in HFD fed mice (Figure 1F), suggesting that the UCP1-dependent thermogenesis of SAT was significantly decreased upon HFD feeding. Considering the increased adipocyte size along with the decreased thermogenic capacity, we speculated that HFD might cause a visceral-like phenotype of SAT. Thus, two sets of marker genes used to characterize classical visceral fat were analyzed in SAT of HFD-fed mice. Compared with mice fed on NCD, both the WAT-selective genes (*Serpina3k*, *Resistin*, *Anxa1*, *Psat*, and *Wdnm1*) and visceral signature genes (*Saa3*, *Wt1*, *Bnc1*, *Agt*, and *Opgn*) were profoundly upregulated in SAT of mice on HFD (Figures 1G and 1H). Taken together, these results suggest that chronic HFD induces the acquisition of both morphological and molecular visceral-like features of SAT, along with the suppressed ability of thermogenesis.

The Expression of SAT PRDM16 Is Downregulated by miR-149-3p in High-Fat Fed Mice

Because *Prdm16* is a critical mediator in SAT thermogenesis and mice lacking *Prdm16* are prone to develop obesity and insulin resistance when placed on HFD,[30] we, therefore, checked *Prdm16* expression in HFD-fed mice. Although only a tendency toward reduced mRNA expression of *Prdm16* was observed in SAT of HFD-fed mice, the protein level of PRDM16 was significantly downregulated (Figures 2A and 2B), confirming our hypothesis that the decreased thermogenic capacity of SAT is associated with impaired PRDM16 function. Given the key role of PRDM16 in the SAT adaptive thermogenesis, restoration of the decreased PRDM16 level might be an efficient way to limit weight gain caused by caloric excess. Interestingly, the inconsistency between the decreased mRNA and protein levels suggested a post-transcriptional regulation of PRDM16 upon HFD feeding, such as miRNAs. In our previous study,[8] we identified that miR-149-3p, which negatively regulated PRDM16 expression by targeting a conserved site of its 3'UTR, was significantly upregulated in SAT of mice on chronic HFD (Figures 2C and S1A). Fluorescent *in situ* hybridization (FISH) assay also confirmed the upregulation of miR-149-3p in HFD adipocytes (Figure 2D). Therefore, the anti-miR-149-3p was directly introduced into the subcutaneous inguinal depot by employing a lentiviral vector. As the schematic diagram shows (Figure 2E), by using multi-point subcutaneous injection, 10^8 lentiviral transducing particles (TU) were inoculated into the inguinal fat of each mouse. The first viral administration was performed on the day prior to HFD feeding, and 6 weeks post-infection, the same

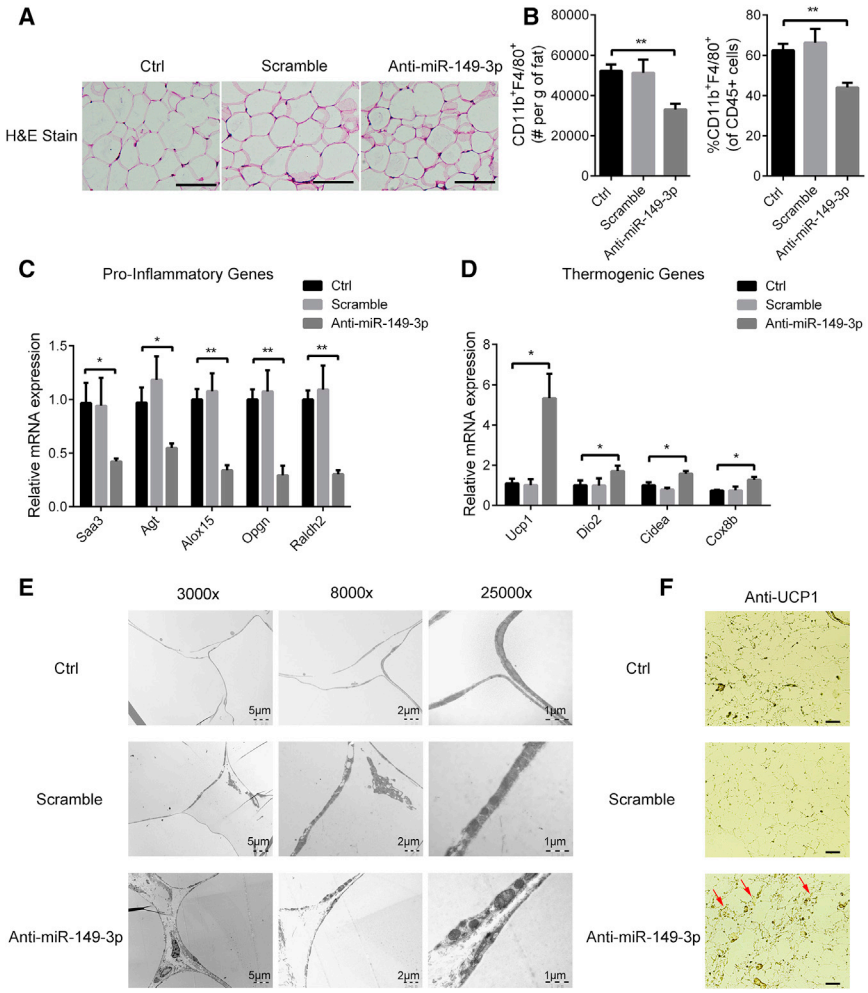

Figure 3. Ablation of miR-149-3p Increases SAT Thermogenesis in High-Fat Fed Mice

(A) H&E staining of SAT infected with LV-scramble or LV-anti-miR-149-3p or PBS. Scale bars: 100 μm. (B) Flow cytometric quantitation of CD11b+F4/80+ macrophages in SAT from mice infected with LV-scramble or LV-anti-miR-149-3p or PBS. (C) Normalized expression of pro-inflammatory genes in the three groups of SAT (n = 8). (D) Normalized expression of thermogenic genes in the three groups of SAT (n = 8). (E) Transmission electron microscopy of SAT from the three groups of mice. Scale bars: 5 μm, 2 μm, 1 μm. (F) Immunohistochemistry for UCP1 protein in sections of SAT from the three groups of mice. Scale bars: 100 μm. *$p < 0.05$, **$p < 0.01$, ***$p < 0.001$.

dose of anti-miR-149-3p was administered again to strengthen the effect. According to the immunohistochemical analysis, 12 weeks post initial treatment, about 70% of inguinal cells were infected as shown by GFP expression (Figure 2F). Significantly decreased fluorescence intensity of miR-149-3p was observed in SAT due to the masking effect of anti-miR-149-3p in the FISH assay (Figure S1B). Inhibition of miR-149-3p robustly upregulated PRDM16 protein level in the subcutaneous inguinal adipose of HFD-fed mice, along with mildly increased mRNA expression (Figures 2G and S2C). Immunofluorescence assay also confirmed the increase of PRDM16 and UCP1 in SAT of HFD-fed mice treated with anti-miR-149-3p (Figure 2H). These results indicate that the expression of SAT PRDM16 is negatively regulated by miR-149-3p when exposed to HFD and suppression of the elevated miR-149-3p can restore PRDM16 protein level.

Ablation of miR-149-3p Increases SAT Thermogenesis in High-Fat-Fed Mice

To assess the influence of miR-149-3p suppression on SAT of HFD-fed mice, we used immunohistochemistry to analyze the morphological change. As shown in Figure 3A, inhibition of SAT miR-149-3p caused a marked decrease in mean adipocyte area of SAT. Then, flow cytometry was used to quantitate the major myeloid and lymphoid subset in the inguinal fat of different groups of mice. Compared to mice treated with scrambled sequence, SAT from anti-miR-149-3p administered mice had a significant decrease in the fraction and number of $CD11b^+F4/80^+$ macrophages (Figure 3B). These observations suggested that the HFD-induced fat cell hypertrophic expansion and macrophage infiltration were ameliorated by anti-miR-149-3p treatment in SAT. Next, we analyzed the expression of a set of pro-inflammatory genes associated with the visceral signature profile. Consistent with previous results, *Saa3*, *Agt*, *Alox15*, *Opgn*, and *Raldh2*, five genes that contribute to inflammation, were all upregulated in HFD-stimulated SAT. However, downregulation of miR-149-3p resulted in profound suppression of these genes (Figure 3C). We next asked whether suppressed miR-149-3p expression in SAT can drive a program of thermogenesis through upregulation PRDM16. As shown in Figure 3E, representative electron micrographs showed that the mitochondria number was elevated in SAT treat with anti-miR-149-3p, indicating the improved metabolic rate. Moreover, the sets of genes associated with the thermogenic program were quantified. As shown in Figure 3D, the suppressed levels of the thermogenic genes (*UCP1*, *Dio2*, *Cidea*, *Cox8b*) were largely restored in SAT of HFD-fed mice by depleting miR-149-3p expression. Immunohistochemical analysis confirmed that the UCP1-expressing fat cells were readily detected in the SAT of miR-149-3p depleted mice, but not in control mice, after 12-week of consuming the HFD (Figure 3F). Collectively, these results suggest that ablation of miR-149-3p decreased the HFD-induced inflammatory gene expressions while promoting the thermogenic program in SAT of mice.

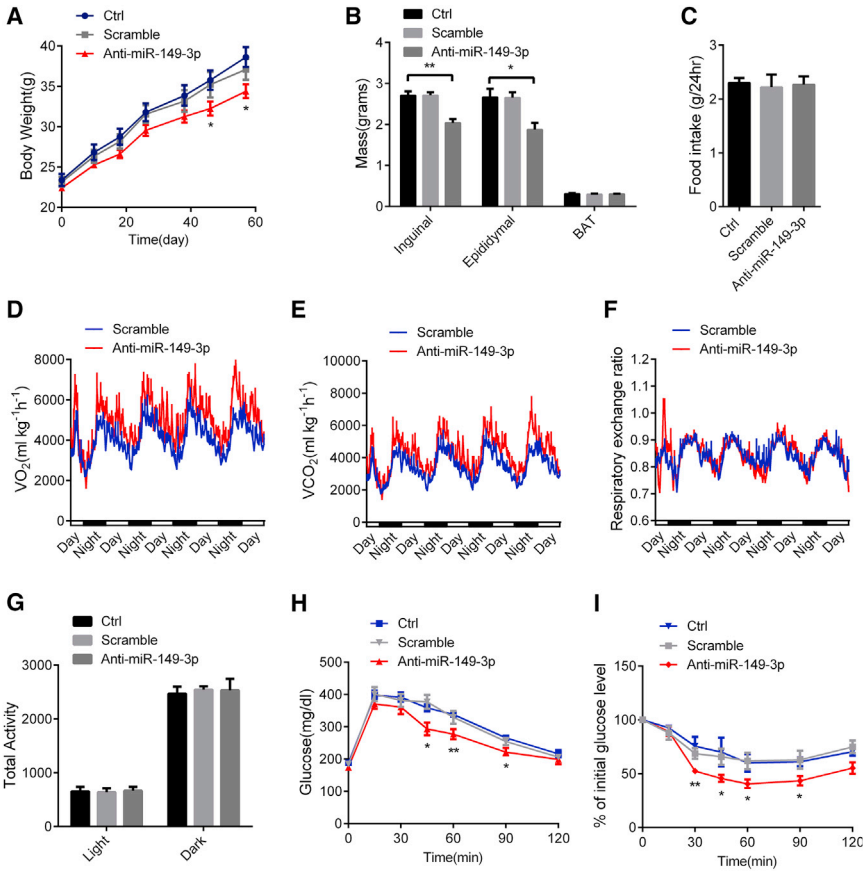

Figure 4. Inhibition of miR-149-3p Protects Mice from Obesity after High-Fat Feeding

(A) Body weights of mice infected with LV-scramble or LV-anti-miR-149-3p or PBS (n = 8). (B) Weights of fat pads from mice infected with LV-scramble or LV-anti-miR-149-3p or PBS (n = 8). (C) Food intake was measured in the three groups of mice after 1 week of high-fat diet (n = 8). (D–F) O_2 consumption (D), CO_2 production (E), and respiratory exchange ratio (F) in LV-scramble or LV-anti-miR-149-3p or PBS infected mice (n = 8). (G) Activity of the three groups of mice after 1 week of HFD at day and night (n = 8). (H and I) Glucose tolerance tests (GTTs) (H) and insulin tolerance tests (ITTs) (I) were performed in the three groups of mice (n = 8). *p < 0.05, **p < 0.01, ***p < 0.001.

SAT Inhibition of miR-149-3p Protects Mice from Obesity and Insulin Resistance upon High-Fat Feeding

In light of the thermogenic effect of anti-miR-149-3p action in SAT, mice were subjected to whole-body metabolic analysis in response to HFD. As shown in Figure 4A, mice treated with anti-miR-149-3p gained significantly less weight than those that received scrambled nucleotides during the 60-day high-fat feeding. Body composition analysis showed that the miR-149-3p-depleted mice had gained less subcutaneous inguinal fat, as well as visceral epididymal mass, consequently resulting in a higher lean/fat mass ratio compared with control groups of mice (Figure 4B). Notably, the reduced body weight gain in anti-miR-149-3p-administered mice was not due to food intake alteration (Figure 4C). However, higher energy expenditure during both day and night cycles was observed in mice with suppressed miR-149-3p (Figures 4D–4F). Importantly, to avoid differences in body weight or composition potentially interfering with the accuracy of metabolic calculations, the energy expenditure was assessed 7 days post high-fat feeding, before the occurrence of body weight change. As shown in Figure 4G, comparable physical activity was also observed between miR-149-3p-depleted mice and control animals. These above results strongly suggest that mice with suppressed SAT miR-149-3p were protected from diet-induced obesity, which resulted from a marked upregulation of energy expenditure and was not linked with physical activity alteration. Because diet-induced obesity is associated with insulin and glucose intolerance, we next performed glucose and insulin tolerance tests on the different groups of mice. Compared to mice treated with anti-miR-149-3p, the control groups of mice showed more pronounced hyperglycemia 45, 60, and 90 min after glucose administration while downregulation of miR-149-3p in SAT resulted in more rapid clearance of glucose (Figure 4H). In addition, high-fat-fed mice with decreased miR-149-3p displayed significantly improved insulin sensitivity relative to control animals, as determined by insulin tolerance test after 12 weeks of HFD (Figure 4I). Together, these observations implicate that decreased miR-149-3p levels in SAT efficiently increases mouse whole-body energy expenditure, which can counteract diet-induced body weight gain and insulin resistance.

Downregulation of miR-149-3p Reverses SAT Visceralization and Metabolic Dysfunction in Obese Mice

Our above results have demonstrated that inhibition of miR-149-3p in SAT can protect mice from obesity and related metabolic dysfunctions. To further determine whether treatment with anti-miR149-3p could be used also as a treatment for obesity, mice were treated with anti-miR149-3p after 12-weeks of HFD from weaning. As indicated in the schematic diagram (Figure 5A), 14 days after multi-point subcutaneous injection of lentiviral vectors either expressing anti-miR-149-3p (5×10^8 TU/mice) or scrambled sequences, metabolic analyses were conducted on both groups of mice. According to immunohistochemical analysis, about 70% of adipocytes in subcutaneous inguinal fat were infected, as indicated by GFP expression (Figure S2A). Compared to scrambled controls, the introduction of anti-miR-149-3p affected neither food intake nor physical activity of mice (Figures 5B and 5C). However, the increased energy expenditure might account for the slight downregulation of body weight and visceral fat mass in the group of mice with decreased level of miR-149-3p (Figures 5D and 5E). The inhibition of miR-149-3p significantly increased PRDM16 and UCP1 levels in SAT, which was highly

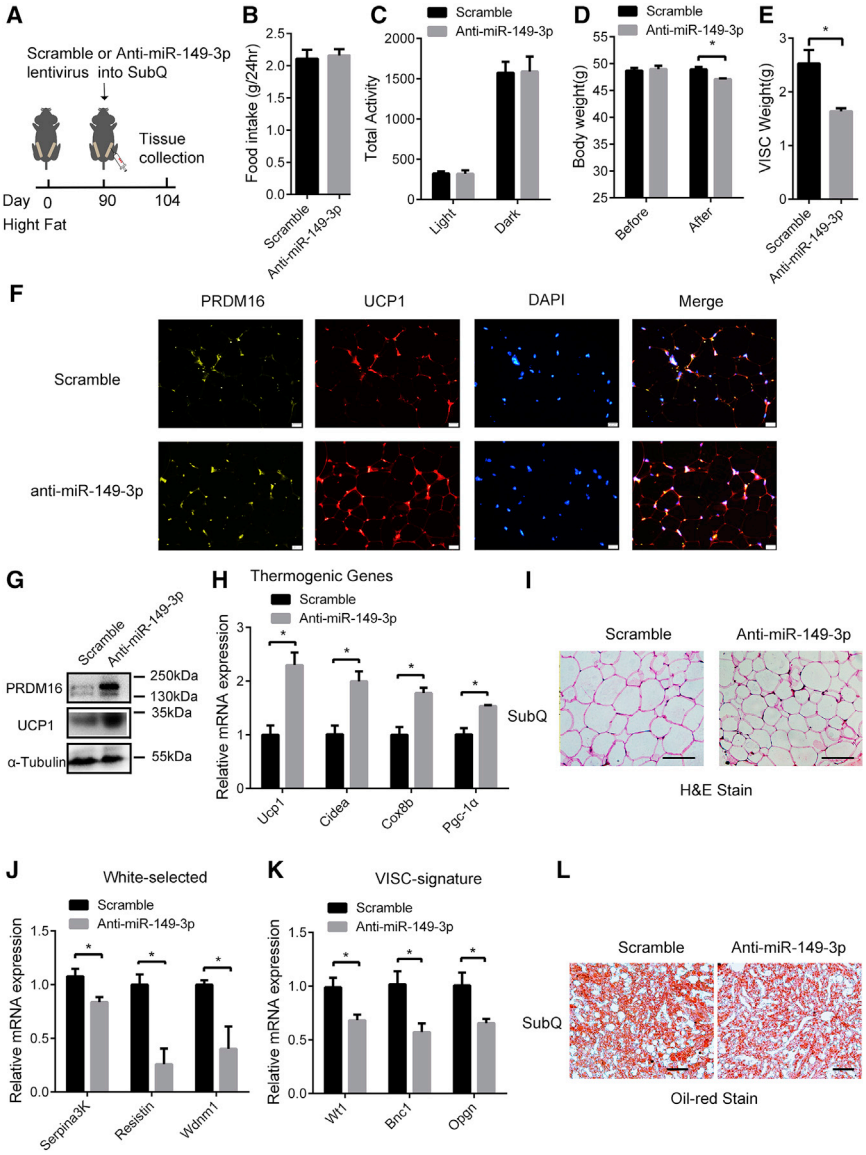

Figure 5. Downregulation of miR-149-3p Reverses Metabolic Dysfunction in Obese Mice

(A–L) After 3 months of HFD, LV-containing scrambled control (scramble) or antisense-miR-149-3p (anti-miR-149-3p) were used for SAT infection in mice (n = 8). (A) Schematic of the experimental protocol. (B–E) Food intake (B), activity (C), body weight (D), and VISC weight (E) of the two groups of mice (n = 8). (F) Immunofluorescence analysis of UCP1 and PRDM16 expression in SAT adipose tissue of mice infected with LV-scramble or LV-miR-149-3p. Scale bars: 20 μm. (G) Western blot analysis of PRDM16 and UCP1 protein levels in SAT infected with LV-scramble or LV-miR-149-3p. (H) Normalized expression of thermogenic genes in SAT infected with LV-scramble or LV-miR-149-3p (n = 8). (I) H&E staining of SAT from mice infected with LV-scramble or LV-miR-149-3p. Scale bars: 100 μm. (J and K) Normalized expression of white-selective genes (J) and visceral-signature genes (K) in LV-infected SAT (n = 8). (L) Oil red O staining of liver from the two groups of mice. Scale bars: 100 μm. *p < 0.05, **p < 0.01, ***p < 0.001.

correlated with browning effects (Figures 5F and 5G). As shown in Figure 5H, the set of thermogenic-associated genes (*Pgc-1α, Cox8b, Cidea*, and *Ucp1*) was robustly elevated by miR-149-3p inhibition. In addition, immunohistochemical analysis showed that the average cell volume was much smaller in SAT, indicating that inhibition of miR-149-3p ameliorated the HFD-induced adipocyte hypertrophic expansion (Figure 5I). Furthermore, two sets of genes (white-selective and visceral-signature) that were drastically increased by high-fat stimulation, were also suppressed in SAT by anti-miR-149-3p treatment (Figures 5J and 5K). Importantly, after 12 weeks of high-fat feeding, severe hepatic steatosis was observed in mice received scramble nucleotides. However, loss of miR-149-3p in SAT profoundly improved hepatic steatosis caused by HFD, as determined by oil red O stained sections of mouse liver from both groups of mice (Figure 5L). Therefore, these results indicate that downregulation of miR-149-3p efficiently induces thermogenesis while suppressing the obesity-induced "visceralization" in SAT, consequently improving whole-body energy expenditure and hepatic steatosis in obese mice.

DISCUSSION

The obesity epidemic has become a serious public health problem. The overconsumption of dietary fat is the main cause of excess body fat accumulation, including the expansion of both visceral and SAT. The current interest in the browning of SAT is mainly related to the possibility that its thermogenic abilities can potentially be recruited to counteract obesity and its related metabolic complications. Our study reveals an important role for miR-149-3p- and *Prdm16*-dependent regulation of the obesity-associated metabolic disorders. Importantly, the reduction of miR-149-3p in SAT partially protects mice from diet-induced weight gain and insulin resistance and may improve hepatic steatosis in obese mice.

Compared to subcutaneous adiposity, which is relatively benign, visceral adiposity has been considered the major culprit in the development of obesity-associated metabolic complications, including type 2 diabetes and liver disease.[2] In recent years, SAT has received great attention due to its extraordinary thermogenic capacity in response to cold exposure or β-adrenergic stimulation.[14] Although it has been noticed that during the onset of obesity, the disrupted catecholamine signals also contribute to excess fat accumulation,[31] the molecular and metabolic changes of SAT when exposed to chronic high-fat feeding have rarely been investigated. Our results showed that

long-term high-fat feeding caused the SAT of mice to acquire partial key properties of visceral fat, including increased lipogenesis and average cell volume, and significantly elevated WAT-selective and visceral-signature genes (Figure 1). Notably, *Saa3*, *Agt*, and *Opgn*, part of the visceral profile, were proinflammatory genes of known functional importance,[32–34] suggesting the increased inflammation in SAT upon high-fat feeding. In addition, we further found that diet-induced obesity was also accompanied by reduced thermogenic capacity of SAT, as most of the thermogenic-related genes (*Pgc-1α*, *Elovl6*, *Cox8b*, and *Cidea*) were decreased, especially the barely detected UCP1 expression. Of note, diet-induced thermogenesis (DIT) has been described as "a myth" due to its vague definition as anything that can dissipate some energy of food eaten.[35,36] Therefore, the significance of DIT for metabolic control is still debated, especially in SAT. In the present study, our data clearly showed that after long-term high-fat feeding (12 weeks), not only was increased mass weight observed, but also, more importantly, thermogenic capacity was markedly blunted in SAT. In line with previous reports that the subcutaneous beige adipose tissue might not play an important role in the UCP1-dependent DIT,[37] our study showed that the readily detected UCP1 protein level in mice fed NCD was decreased significantly when exposed to chronic high-fat feeding. Partial acquisition of visceral-like features and suppressed thermogenicability, the beneficial effect of SAT was largely impaired upon chronic high-fat feeding. Therefore, our data strongly suggested that restoring the suppressed function of SAT, especially the thermogenic program, might confer beneficial effects on diet-induced adiposity and insulin resistance.

It is still unclear whether the HFD-induced visceral-like phenotype of SAT is causally related to its repressed thermogenic ability, however, this observation is reminiscent of the molecular and morphological pattern seen in Adipo-PRDM16 knockout mice. As the master transcription factor that promotes thermogenesis in SAT, loss of PRDM16 not only blunts the thermogenic program characteristic of SAT but also induces its acquisition of some of the deleterious features of visceral fat,[17] which is consistent with our observations in the SAT of mice on chronic high-fat feeding. Adipo-PRDM16 knockout had minimal effects on BAT but markedly inhibited "browning" of SAT. Furthermore, adipo-PRDM16 knockout mice gained more weight on a HFD, which might be due to the loss of PRDM16 in SAT. As expected, we found that the PRDM16 protein level was sharply decreased in SAT upon HFD, indicating that the downregulated PRDM16 might account for the lost beneficial effect of SAT (Figure 2). According to previous studies, mice with more beige adipocytes have been found to be protected from metabolic diseases. Overexpression of *Prdm16* in adipose lineages resulted in significant "browning" of SAT along with increased energy expenditure, which improved glucose metabolism and insulin sensitivity. Meanwhile aP2-PRDM16 transgenic mice displayed slightly increased lean mass on a chow diet, and the thermogenic gene expression was robustly increased in SAT while the morphological appearance of the SAT was more BAT-like.[15] However, transgenic expression of *Prdm16* in adipose tissue using the aP2 promoter did not increase the levels of thermogenic genes in visceral fat and interscapular BAT (iBAT). Therefore, the benefits of *Prdm16* overexpression in adipose tissue might depend on its effect on SAT. However, there is still a lack of direct evidence that *Prdm16* also plays an important anti-obesity and anti-diabetic role in an obese background. Our study is the first to prove that upregulation of *Prdm16* in SAT of the diet-induced obese mice can ameliorate body weight gain and improve system insulin sensitivity (Figure 5). Thus, signaling molecules that could upregulate *Prdm16* may represent new targets for clinical applications.

Researchers have identified that PPAR agonists, such as Rosiglitazone, could induce the thermogenic program in SAT through stabilizing PRDM16 protein, however, more mechanistic studies are required due to the severe side effects of the Glitazones *in vivo*. miRNAs have been shown to play crucial roles in gene regulation during adipogenesis including the browning of SAT,[22,25] thus representing promising therapeutic targets for metabolic diseases. The myomiR-133, proinflammatory miR-155, and miR-34a have been reported to negatively regulate the browning process of SAT, whereas miR-196a, miR-27, and miR-378 were identified as positive regulators of cold-induced thermogenesis.[22–24,26,38,39] In this study, we observed a robust upregulation of miR-149-3p in SAT of HFD-fed mice. Because we have demonstrated that *Prdm16* is a direct target of miR-149-3p, we showed here that the inhibition of miR-149-3p in SAT of mice with an HFD resulted in a significant increase in PRDM16 protein level, as well as SAT thermogenesis and whole-body energy expenditure, with no alteration in food intake and physical activity. More importantly, depletion of miR-149-3p led to improved glucose tolerance and insulin sensitivity, while decreasing the infiltration of macrophages in SAT, and liver steatosis in mice fed a HFD (Figures 3 and 4).

In addition, it has recently been shown that beige fat may also secrete endocrine factors to modulate systemic metabolism. For instance, beige fat can secrete interleukin-6 to regulate hepatic glucose and lipid metabolism.[40] As a critical transcriptional factor, PRDM16 can powerfully regulate beige adipocyte differentiation and secretion; for example, Slit2-C secreted by SAT of aP2-PRDM16 transgenic mice promotes SAT thermogenesis.[41] Therefore, it may be worth exploring whether SAT activated by PRDM16 secretes endocrine factors to ameliorate metabolic disorders.

In summary, we have provided direct evidence of the anti-obesity and anti-diabetic effect of *Prdm16* in the obese background for the first time. Our study also revealed an important mechanism of miR-149-3p- and *Prdm16*-dependent regulation of energy expenditure upon chronic high-fat feeding, indicating that SAT miR-149-3p can serve as a therapeutic target to defend against diet-induced obesity and metabolic dysfunctions.

MATERIALS AND METHODS

Reagents and Antibodies

The MystiCq microRNA qPCR Assay (cat#MIRRM02) and TRIzol reagent (cat#T9424) were purchased from Sigma (Deisenhogfen, Germany). RIPA buffer (cat#P0013B), protease, and phosphatase inhibitor cocktail (cat#P1048) were purchased from Beyotime

(Shanghai, China). For western blotting, anti-PRDM16 antibody (cat#AF6295) was purchased from R&D Systems (Tustin, CA, USA), anti-UCP1 antibody (cat#14670) was purchased from Cell Signaling Technologies (Danvers, MA, USA), and anti-α-tubulin (cat#sc-53646) was purchased from Santa Cruz Biotechnology (Santa Cruz, CA, USA). For flow cytometry, anti-CD11b (cat#101207), anti-CD45 (cat#103121), and anti-F4/80 (cat#123115) were purchased from BioLegend (San Diego, CA, USA). Anti-UCP1 used for immunohistochemistry was purchased from Abcam (Cambridge, MA, USA).

Animals

All animal experiments were performed in accordance with the NIH Guide for the Care and Use of Laboratory Animals and were approved by the Animal Care Committee of Nanjing University. Male C57BL/6J (B6) mice were obtained from the Model Animal Research Center of Nanjing University. Adult C57 mice were divided into three groups. The three groups were injected with PBS, scrambled lentivirus, or miR-149 inhibiting lentivirus in inguinal adipose tissue *in vivo*. The method used for local injection of lentivirus was described earlier.[8] Lentivirus packaged with mouse miR-149-3p antisense and Scramble were purchased from GenePharma (Shanghai, China). 1% pentobarbital sodium was used to anaesthetize mice. In both sides of the inguinal parts, a short incision was made. For protocol one, 50 μL of lentiviral particles (1×10^9 TU/mL, 100 μL/mouse) were injected directly into the inguinal adipose tissues of 4-week-old C57BL/6J mice. After injection, the incisions were sutured and mice were fed *ad libitum* HFD (60% energy in kcal from fat) (Research Diets, New Brunswick, NJ, USA). The virus-infected mice were injected once more after 30 days later, and then sacrificed 60 days later. For protocol two, 150 μL of lentiviral particles (1×10^9 TU/mL, 300 μL/mouse) were injected directly into the inguinal adipose tissues of mice on high-fat diet for 3 months. After 15 days, the mice were sacrificed.

Design of Lentiviral Vectors

The anti-miR-149-3p oligonucleotide sequence, which is fully complementary to the mature miR-149-3p (5′-GCACCGCCCCCG TCCCTCCCTC-3′), was designed. For general anti-miRNA oligonucleotide (AMO) designing, it is required that the AMO binds with high affinity to the miRNA "seed region," which spans bases 2–8 from the 5′ end of the miRNA. Here, the anti-miR-149-3p we employed was fully complementary to the mature miR-149-3p to increase binding affinity. The scramble sequence packaged into lentiviruses was 5′-TTCTCCGAACGTGTCACGT-3′. Then we purchased the GFP-expressing lentiviral vector LV3-pGLV-H1-GFP+Puro from GenePharma. The previously designed anti-miR-149-3p sequence was cloned into the lentiviral vector by GenePharma.

Immunohistochemical Staining

For immunohistochemical staining, inguinal adipose tissues were fixed in 4% paraformaldehyde for 24 h and then embedded in OCT. Cryostat sections of the inguinal adipose tissues were stained with DAPI (Eugene, Oregon, USA). The infected cells expressing GFP were visualized by immunofluorescence microscopy.

For UCP1 immunohistochemistry, 4% paraformaldehyde was used to fix inguinal adipose tissues for 24 h and then issues were embedded in paraffin. Slides (5 μm in thickness) were deparaffinized and incubated with rabbit polyclonal UCP1 antibody (1:500; Abcam, Cambridge, MA, USA) overnight at 4°C. Signals were amplified using 1:500 goat anti-rabbit immunoglobulin G horseradish peroxidase-linked antibody (Vector Laboratories, Burlingame, CA, USA) with the ABC kit (Vector Laboratories, Burlingame, CA, USA) and DAB substrate (Vector Laboratories, Burlingame, CA, USA). For H&E staining, slides were stained with eosin and hematoxylin (Nanjing Jiancheng Bioengineering Institute, Nanjing, China).

Oil Red O Staining

Livers were fixed in 4% paraformaldehyde for 24 h and then embedded in OCT. Multiple slides (8 μm in thickness) were prepared and then rinsed with 70% ethanol for 2 min. Then oil red O (Sigma, Deisenhogfen, Germany) was used to stain the lipids for 15 min and the slides were rinsed with 75% ethanol for 5 min. The slides were washed with PBS and imaged immediately.

Western Blotting and Gene Expression

For western blot analysis, tissues were extracted with RIPA buffer (Beyotime, Shanghai, China) supplemented with phosphatase and protease inhibitor cocktail (Beyotime, Shanghai, China). Proteins were resolved by 10% SDS-PAGE, and then probed with antibodies against PRDM16, UCP1, α-tubulin.

Total RNA from inguinal adipose tissues was extracted using the TRIzol method. For qPCR analysis, oligo d(T)18 primers (TaKaRa, Dalian, China) were used for reverse transcription of mRNA. To generate fluorescence, we used SYBR Green dye (Ambion, Carlsbad, CA, USA) combined with gene-specific primer pairs for mRNA quantification. Then the relative mRNA expression was normalized with 36B4 using the ΔΔCt method. miR-149-3p expression was verified by qPCR using the MystiCq microRNA qPCR Assay (Sigma, Deisenhogfen, Germany).

Flow Cytometry

Inguinal adipose tissue was excised and digested with collagenase type II (Sigma, Deisenhogfen, Germany). A 40 mm sieve was used to filter the cell suspensions, and after centrifugation at 450 g for 10 min the SVF was collected. To quantify macrophages, we stained SVF cells with anti-CD11b (BioLegend, San Diego, CA, USA), CD45 (BioLegend, San Diego, CA, USA) and F4/80 (BioLegend, San Diego, CA, USA). LSRIIinstrument (BD Bioscience, New Jersey, USA) and FlowJo software (single cell analysis, version 7.6.1, Oregon) were used to analyze the results.

Glucose Tolerance and Insulin Tolerance Tests

For glucose tolerance tests, mice were fasted for 14 h and then intraperitoneally (i.p.) injected with dextrose (1 g/kg body weight). For insulin tolerance tests, mice were fasted for 6 h and then insulin (1 units/kg body weight) was administered by i.p. injection. For both glucose tolerance and insulin tolerance tests, a standard glucometer

was used to measure glucose levels in tail blood at 0 min, 15 min, 30 min, 60 min, 90 min, and 120 min following injection.

Statistics

All data were analyzed in GraphPad Prism 6.0 (GraphPad Software) with two-tailed Student's t tests. p values less than 0.05 were considered statistically significant: $^{*}p \leq 0.05$, $^{**}p \leq 0.005$, $^{***}p \leq 0.001$. All values were presented as the mean ± SEM.

SUPPLEMENTAL INFORMATION

Supplemental Information can be found online at https://doi.org/10.1016/j.omtn.2019.07.024.

AUTHOR CONTRIBUTIONS

S.Z. and X.J. designed the study, performed experiments, and analyzed data. S.Z., S.G., G.S., Y.S., Z.W., C.S., P.D., Y.T., F.H., and H.C. performed experiments and analyzed data. K.Z. and C.-Y.Z. interpreted data and contributed to the discussion. Y.Z., I.S., S.Z., J.L., and X.J. wrote the manuscript.

CONFLICTS OF INTEREST

The authors declare no competing interests.

ACKNOWLEDGMENTS

We are grateful to Dr. Bruce M. Spiegelman of Harvard Medical School, for kindly providing us with the primer sequences of visceral-selective genes. This work was supported by grants from the National Natural Science Foundation of China (31972912, 31771666, and 31741066) and the Fundamental Research Funds for the Central Universities (020814380087, 020814380094, and 0208131230).

REFERENCES

1. Kopelman, P.G. (2000). Obesity as a medical problem. Nature *404*, 635–643.
2. Després, J.P., and Lemieux, I. (2006). Abdominal obesity and metabolic syndrome. Nature *444*, 881–887.
3. Kahn, S.E., Hull, R.L., and Utzschneider, K.M. (2006). Mechanisms linking obesity to insulin resistance and type 2 diabetes. Nature *444*, 840–846.
4. Van Gaal, L.F., Mertens, I.L., and De Block, C.E. (2006). Mechanisms linking obesity with cardiovascular disease. Nature *444*, 875–880.
5. The Lancet (2017). The link between cancer and obesity. Lancet *390*, 1716.
6. Hu, S., Wang, L., Yang, D., Li, L., Togo, J., Wu, Y., Liu, Q., Li, B., Li, M., Wang, G., et al. (2018). Dietary Fat, but Not Protein or Carbohydrate, Regulates Energy Intake and Causes Adiposity in Mice. Cell Metab *28*, 415–431 e414.
7. Cannon, B., and Nedergaard, J. (2008). Developmental biology: Neither fat nor flesh. Nature *454*, 947–948.
8. Ding, H., Zheng, S., Garcia-Ruiz, D., Hou, D., Wei, Z., Liao, Z., Li, L., Zhang, Y., Han, X., Zen, K., et al. (2016). Fasting induces a subcutaneous-to-visceral fat switch mediated by microRNA-149-3p and suppression of PRDM16. Nat. Commun. *7*, 11533.
9. Villarroya, F., Cereijo, R., Gavaldà-Navarro, A., Villarroya, J., and Giralt, M. (2018). Inflammation of brown/beige adipose tissues in obesity and metabolic disease. J. Intern. Med. *284*, 492–504.
10. Harms, M., and Seale, P. (2013). Brown and beige fat: development, function and therapeutic potential. Nat. Med. *19*, 1252–1263.
11. Poret, J.M., Souza-Smith, F., Marcell, S.J., Gaudet, D.A., Tzeng, T.H., Braymer, H.D., Harrison-Bernard, L.M., and Primeaux, S.D. (2018). High fat diet consumption differentially affects adipose tissue inflammation and adipocyte size in obesity-prone and obesity-resistant rats. Int. J. Obes. *42*, 535–541.
12. Wu, J., Cohen, P., and Spiegelman, B.M. (2013). Adaptive thermogenesis in adipocytes: is beige the new brown? Genes Dev. *27*, 234–250.
13. Vitali, A., Murano, I., Zingaretti, M.C., Frontini, A., Ricquier, D., and Cinti, S. (2012). The adipose organ of obesity-prone C57BL/6J mice is composed of mixed white and brown adipocytes. J. Lipid Res. *53*, 619–629.
14. van der Lans, A.A., Hoeks, J., Brans, B., Vijgen, G.H., Visser, M.G., Vosselman, M.J., Hansen, J., Jörgensen, J.A., Wu, J., Mottaghy, F.M., et al. (2013). Cold acclimation recruits human brown fat and increases nonshivering thermogenesis. J. Clin. Invest. *123*, 3395–3403.
15. Seale, P., Conroe, H.M., Estall, J., Kajimura, S., Frontini, A., Ishibashi, J., Cohen, P., Cinti, S., and Spiegelman, B.M. (2011). Prdm16 determines the thermogenic program of subcutaneous white adipose tissue in mice. J. Clin. Invest. *121*, 96–105.
16. Chi, J., and Cohen, P. (2016). The Multifaceted Roles of PRDM16: Adipose Biology and Beyond. Trends Endocrinol. Metab. *27*, 11–23.
17. Cohen, P., Levy, J.D., Zhang, Y., Frontini, A., Kolodin, D.P., Svensson, K.J., Lo, J.C., Zeng, X., Ye, L., Khandekar, M.J., et al. (2014). Ablation of PRDM16 and beige adipose causes metabolic dysfunction and a subcutaneous to visceral fat switch. Cell *156*, 304–316.
18. Ohno, H., Shinoda, K., Spiegelman, B.M., and Kajimura, S. (2012). PPARγ agonists induce a white-to-brown fat conversion through stabilization of PRDM16 protein. Cell Metab. *15*, 395–404.
19. Bartel, D.P. (2004). MicroRNAs: genomics, biogenesis, mechanism, and function. Cell *116*, 281–297.
20. Mysore, R., Ortega, F.J., Latorre, J., Ahonen, M., Savolainen-Peltonen, H., Fischer-Posovszky, P., Wabitsch, M., Olkkonen, V.M., Fernández-Real, J.M., and Haridas, P.A.N. (2017). MicroRNA-221-3p Regulates Angiopoietin-Like 8 (ANGPTL8) Expression in Adipocytes. J. Clin. Endocrinol. Metab. *102*, 4001–4012.
21. Mori, M.A., Thomou, T., Boucher, J., Lee, K.Y., Lallukka, S., Kim, J.K., Torriani, M., Yki-Järvinen, H., Grinspoon, S.K., Cypess, A.M., and Kahn, C.R. (2014). Altered miRNA processing disrupts brown/white adipocyte determination and associates with lipodystrophy. J. Clin. Invest. *124*, 3339–3351.
22. Pan, D., Mao, C., Quattrochi, B., Friedline, R.H., Zhu, L.J., Jung, D.Y., Kim, J.K., Lewis, B., and Wang, Y.X. (2014). MicroRNA-378 controls classical brown fat expansion to counteract obesity. Nat. Commun. *5*, 4725.
23. Sun, L., and Trajkovski, M. (2014). MiR-27 orchestrates the transcriptional regulation of brown adipogenesis. Metabolism *63*, 272–282.
24. Chen, Y., Siegel, F., Kipschull, S., Haas, B., Fröhlich, H., Meister, G., and Pfeifer, A. (2013). miR-155 regulates differentiation of brown and beige adipocytes via a bistable circuit. Nat. Commun. *4*, 1769.
25. Sun, L., Xie, H., Mori, M.A., Alexander, R., Yuan, B., Hattangadi, S.M., Liu, Q., Kahn, C.R., and Lodish, H.F. (2011). Mir193b-365 is essential for brown fat differentiation. Nat. Cell Biol. *13*, 958–965.
26. Mori, M., Nakagami, H., Rodriguez-Araujo, G., Nimura, K., and Kaneda, Y. (2012). Essential role for miR-196a in brown adipogenesis of white fat progenitor cells. PLoS Biol. *10*, e1001314.
27. Haykowsky, M.J., Nicklas, B.J., Brubaker, P.H., Hundley, W.G., Brinkley, T.E., Upadhya, B., Becton, J.T., Nelson, M.D., Chen, H., and Kitzman, D.W. (2018). Regional Adipose Distribution and its Relationship to Exercise Intolerance in Older Obese Patients Who Have Heart Failure With Preserved Ejection Fraction. JACC Heart Fail. *6*, 640–649.
28. Kissebah, A.H., Vydelingum, N., Murray, R., Evans, D.J., Hartz, A.J., Kalkhoff, R.K., and Adams, P.W. (1982). Relation of body fat distribution to metabolic complications of obesity. J. Clin. Endocrinol. Metab. *54*, 254–260.
29. Moon, H.U., Ha, K.H., Han, S.J., Kim, H.J., and Kim, D.J. (2018). The Association of Adiponectin and Visceral Fat with Insulin Resistance and β-Cell Dysfunction. J. Korean Med. Sci. *34*, e7.
30. Park, H., He, A., Tan, M., Johnson, J.M., Dean, J.M., Pietka, T.A., Chen, Y., Zhang, X., Hsu, F.F., Razani, B., et al. (2019). Peroxisome-derived lipids regulate adipose thermogenesis by mediating cold-induced mitochondrial fission. J. Clin. Invest. *129*, 694–711.

31. Reilly, S.M., and Saltiel, A.R. (2017). Adapting to obesity with adipose tissue inflammation. Nat. Rev. Endocrinol. *13*, 633–643.

32. Pinheiro, T.A., Barcala-Jorge, A.S., Andrade, J.M.O., Pinheiro, T.A., Ferreira, E.C.N., Crespo, T.S., Batista-Jorge, G.C., Vieira, C.A., Lelis, D.F., et al. (2017). Obesity and malnutrition similarly alter the renin–angiotensin system and inflammation in mice and human adipose. J. Nutr. Biochem. *48*, 74–82.

33. Aronis, K.N., Foo, J.P., Chamberland, J.P., and Mantzoros, C.S. (2012). Secretion patterns of circulating osteoprotegerin and response to acute and chronic energy deprivation in young healthy adults. J. Clin. Endocrinol. Metab. *97*, 2765–2772.

34. Ather, J.L., and Poynter, M.E. (2018). Serum amyloid A3 is required for normal weight and immunometabolic function in mice. PLoS ONE *13*, e0192352.

35. Kozak, L.P. (2010). Brown fat and the myth of diet-induced thermogenesis. Cell Metab. *11*, 263–267.

36. Maxwell, G.M., Nobbs, S., and Bates, D.J. (1987). Diet-induced thermogenesis in cafeteria-fed rats: a myth? Am. J. Physiol. *253*, E264–E270.

37. von Essen, G., Lindsund, E., Cannon, B., and Nedergaard, J. (2017). Adaptive facultative diet-induced thermogenesis in wild-type but not in UCP1-ablated mice. Am. J. Physiol. Endocrinol. Metab. *313*, E515–E527.

38. Yin, H., Pasut, A., Soleimani, V.D., Bentzinger, C.F., Antoun, G., Thorn, S., Seale, P., Fernando, P., van Ijcken, W., Grosveld, F., et al. (2013). MicroRNA-133 controls brown adipose determination in skeletal muscle satellite cells by targeting Prdm16. Cell Metab. *17*, 210–224.

39. Sun, Y.M., Qin, J., Liu, S.G., Cai, R., Chen, X.C., Wang, X.M., and Pang, W.J. (2017). PDGFRα Regulated by miR-34a and FoxO1 Promotes Adipogenesis in Porcine Intramuscular Preadipocytes through Erk Signaling Pathway. Int. J. Mol. Sci. *18*, 18.

40. Scheja, L., and Heeren, J. (2016). Metabolic interplay between white, beige, brown adipocytes and the liver. J. Hepatol. *64*, 1176–1186.

41. Svensson, K.J., Long, J.Z., Jedrychowski, M.P., Cohen, P., Lo, J.C., Serag, S., Kir, S., Shinoda, K., Tartaglia, J.A., Rao, R.R., et al. (2016). A Secreted Slit2 Fragment Regulates Adipose Tissue Thermogenesis and Metabolic Function. Cell Metab. *23*, 454–466.